Available online at www.sciencedirect.com
ScienceDirect
Journal of Sound and Vibration 299 (2007) 822–838
JOURNAL OF SOUND AND VIBRATION
www.elsevier.com/locate/jsvi

Experimental demonstration of transient resonance capture in a system of two coupled oscillators with essential stiffness nonlinearity

Gaëtan Kerschen[a,*], D. Michael McFarland[b], Jeffrey J. Kowtko[b], Young S. Lee[b], Lawrence A. Bergman[b], Alexander F. Vakakis[b,c,d]

[a]*Aerospace and Mechanical Engineering Department, University of Liège, Chemin des Chevreuils 1 (B52/3), B-4000 Liège, Belgium*
[b]*Department of Aerospace Engineering, University of Illinois at Urbana-Champaign, USA*
[c]*Division of Mechanics, National Technical University of Athens, Greece*
[d]*Department of Mechanical and Industrial Engineering, University of Illinois at Urbana Champaign, USA*

Received 19 October 2005; received in revised form 5 July 2006; accepted 16 July 2006
Available online 2 October 2006

Abstract

The purpose of this paper is to report an experimental study of transient resonance capture that may occur in a system of two coupled oscillators with essential (i.e., nonlinearizable) nonlinearity. It is shown that during transient resonance capture the two oscillators are in a state of resonance, the frequency of which varies with time, which leads to targeted nonlinear energy transfer. Further evidence of resonance capture is a non-time-like behavior of the phase difference between the oscillators; this quantity is monitored using the Hilbert transform or the Huang–Hilbert transform in the case of multifrequency response signals.

1. Introduction

Resonances that are most commonly considered in the dynamical systems literature correspond to specific frequencies of oscillation; that is, resonance of a mode shape at its natural frequency [1] or of nonlinear modes in internal resonance [2]. However, previous studies (see, e.g., Refs. [3–5]) have indicated that other kinds of resonances, characterized by varying frequencies of oscillation, termed *resonance captures*, may also be encountered.

During the last 10 years, resonance capture phenomena have received increasing attention in the literature (see, e.g., Refs. [6–23]). An example of sustained resonance capture (SRC) is given in Ref. [6], in which a system composed of an unbalanced rotor attached to an elastic support and driven by a constant torque is considered. The main characteristic of SRC is that the frequency of the sustained resonance shifts depending

*Corresponding author. Tel.: +32 4 366 90 98; fax: +32 4 366 48 56.
E-mail addresses: g.kerschen@ulg.ac.be (G. Kerschen), dmmcf@uiuc.edu (D.M. McFarland), kowtko@uiuc.edu (J.J. Kowtko), yslee4@uiuc.edu (Y.S. Lee), lbergman@uiuc.edu (L.A. Bergman), vakakis@central.ntua.gr, , avakakis@uiuc.edu (A.F. Vakakis).

0022-460X/$ - see front matter © 2006 Elsevier Ltd. All rights reserved.
doi:10.1016/j.jsv.2006.07.029

upon the system parameters, for example, the torque applied to the rotor or the amount of damping present in the system in the case of Ref. [6]. This study also underlined that, if the applied torque is too large, SRC is no longer experienced in the system; more precisely, the existence of SRC is conditional upon the system parameters.

In Refs. [7,8], transient resonance capture (TRC) was observed during the free response of a single-degree-of-freedom oscillator coupled to an essentially nonlinear attachment, termed a *nonlinear energy sink* (NES). During TRC, the oscillators are locked into a resonance with identical but time-varying frequency, and its main feature is that the system trajectories approach and evolve along the resonance manifold for a short interval of time before escape [9]. In Refs. [7,8], the frequency decreased with time due to the hardening characteristic of the nonlinearity, and TRC became manifest only above a threshold of the input energy. In addition to 1:1 TRC, higher-order TRCs (e.g., 1:2 or 1:3 TRCs) were observed in a similar system [10,11]; in these studies the two oscillators were locked into transient resonance with different frequencies. Each of the individual frequencies varied with time but their ratio remained constant. A cascade of TRCs, transient resonances with a number of nonlinear modes, was reported in Ref. [12] for a multi-degree-of-freedom linear system weakly coupled to an NES.

In the references cited above, resonance captures originate from the presence of components that may adapt their frequency and may lead to interesting dynamical phenomena. Some other studies focused more on the theoretical aspects of resonance capture. For instance, in Ref. [13], the authors explained that resonance capture can be interpreted conceptually in terms of a slowly varying separatrix in phase space, which allows the dynamical flow to pass across it. Likewise, the flow can escape from resonance capture by again crossing the separatrix. They also proposed an energy method and a perturbation method for estimating the initial conditions that lead to resonance capture.

Resonance capture now enjoys various applications, including spacecraft dynamics [14], analysis of the dynamics of charged particles in non-homogeneous electromagnetic fields [17], celestial mechanics [18], energy exchanges between coupled oscillators (also called nonlinear energy pumping [7,8,10–12,19,20,22,23]) and elimination of limit cycles [21].

The present study is the continuation of the experimental developments reported in Refs. [22,23]. In Ref. [22], complex and vigorous energy transfers from the linear oscillator to the NES, leading to large fractions of energy dissipated in the NES, were reported. In Ref. [23], the two basic mechanisms governing these energy transfers were highlighted, namely the excitation of a transient bridging orbit—resulting in a nonlinear beating phenomenon—and resonance capture into a 1:1 resonance manifold—resulting in irreversible energy flow from the primary system to the NES—with the former mechanism triggering the latter. In this study, the emphasis is put upon the 1:1 TRC. Specifically, it is shown that during TRC the two oscillators are in a state of resonance capture with decreasing frequency, which leads to targeted nonlinear energy transfers. Further evidence of resonance capture is a non-time-like behavior of the phase difference between the oscillators; this quantity is monitored using the Hilbert transform or the Huang–Hilbert transform in the case of multifrequency response signals.

2. Experimental setup

2.1. Description of the experimental fixture

The system considered herein is composed of a linear oscillator, termed the primary system, weakly coupled to an essentially nonlinear (nonlinearizable) oscillator, termed the NES, and is described by the equations

$$\begin{aligned} M\ddot{y} + c_1\dot{y} + c_{12}(\dot{y} - \dot{v}) + k_1 y + k_{12}(y - v) = 0, \\ m\ddot{v} + c_2\dot{v} + c_{12}(\dot{v} - \dot{y}) + Cv^3 + k_{12}(v - y) = 0. \end{aligned} \tag{1}$$

Variables y and v refer to the displacement of the primary system and of the NES, respectively. Weak coupling is assured by requiring that $k_{12} \ll k_1$. The nonlinear coefficient C is treated as an $O(1)$ quantity. Provided the input energy is high enough, these equations represent a strongly nonlinear system.

The experimental fixture built to examine the energy transfers in the two-degree-of-freedom system described by Eqs. (1) is depicted in Fig. 1. A schematic of the system is provided in Fig. 2, detailing major components. The fixture comprised two cars made of aluminum angle stock which were supported on a straight air track [see Fig. 3(c)]. The primary system mass M was grounded by means of the linear spring k_1 [see Figs. 3(a) and (b)], and the NES mass m was connected to the primary system by means of a weak coupling stiffness k_{12}. An essential cubic nonlinearity C was realized by a thin wire with no pretension. Viscoelastic tape was added to the coupling spring, realizing the damping constant c_{12}. Teflon coating was attached to the underside of the cars to reduce any friction that might occur while the cars were in motion. As a result, the damping constants c_1 and c_2 were much smaller than c_{12}. A long-stroke electrodynamic shaker provided a controlled and repeatable short force pulse to the primary system (i.e., the left car in the upper picture in Fig. 1). A representative broadband input force is shown in Fig. 4.

The response of both oscillators was measured using accelerometers. Estimates of the corresponding velocity and displacement were obtained by integrating the measured acceleration. The resulting signals were then high-pass filtered to remove the spurious components introduced by the integration procedure.

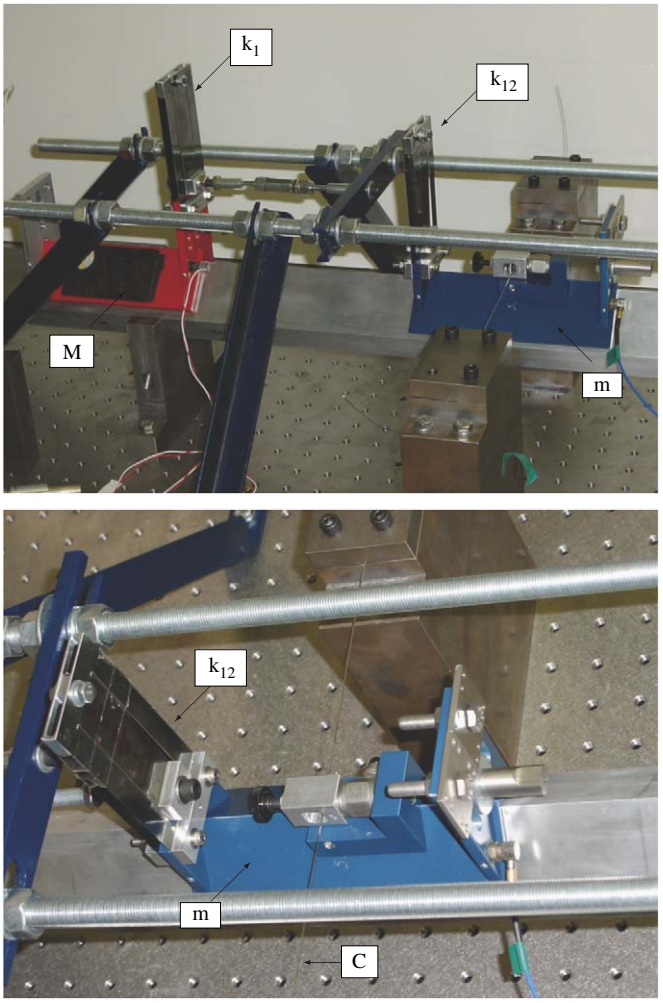

Fig. 1. Upper picture: experimental fixture; lower picture: close-up of the NES.

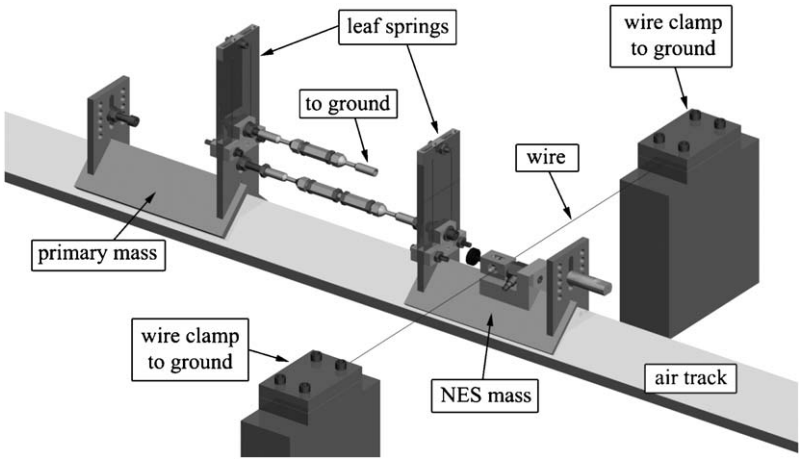

Fig. 2. Schematic of the experimental fixture.

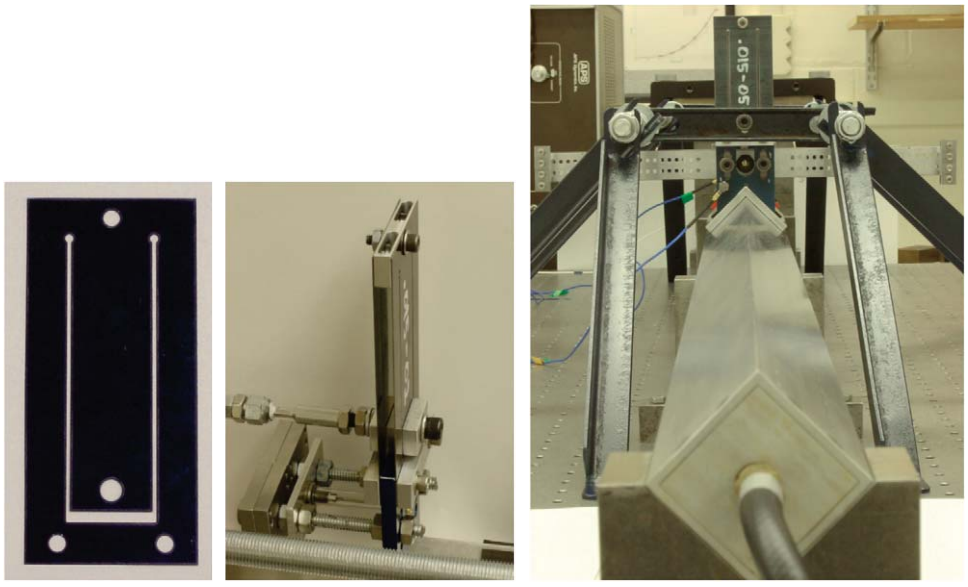

(a) (b) (c)

Fig. 3. (a) Leaf spring; (b) leaf spring assembly attached to car; (c) end view of air track with resting car.

2.2. System identification

The goal of system identification is to exploit input and output measurements performed on the structure using vibration sensing devices in order to estimate all the parameters in the equation of motion (1). Prior to system identification, the primary system and the NES were weighed, and their masses were found to be $M = 0.7348\,\text{kg}$ and $m = 0.4734\,\text{kg}$, respectively.

System identification was carried out in three separate steps:

- The primary system was disconnected from the NES, and modal analysis was performed on the disconnected primary system. The natural frequency and the viscous damping ratio were estimated to be 5.70 Hz and 0.17%, respectively. Because the mass of the primary system was known, the stiffness and damping parameters k_1 and c_1 were easily deduced from this modal analysis.

- The wire was disconnected, and a modal analysis of the coupled linear system was performed. This resulted in estimates of the weak coupling stiffness k_{12} and the damping constants c_{12} and c_2.
- The NES was disconnected from the primary system with the aim of estimating the nonlinear coefficient C. To this end, the restoring force surface method [24] was employed. In essence, Newton's second law was applied to the second car

$$f_{\mathrm{NL}}(v,\dot{v}) = p - m\ddot{v} \tag{2}$$

where $f_{\mathrm{NL}}(v,\dot{v})$ is the restoring force and p the external force (for simplicity, the temporal dependence is omitted). Eq. (2) shows that the time history of the restoring force can be calculated directly from the measurement of the acceleration and the external force and from the knowledge of the mass. The model

$$f_{\mathrm{NL}}(v,\dot{v}) = c_2\dot{v} + Cv^3 + C_{\mathrm{lin}}v \tag{3}$$

was then fitted to the estimate of the restoring force. For greater flexibility, the functional form of the nonlinearity also included a linear spring C_{lin}. Finally, least-squares parameter estimation was used to obtain the values of the coefficients C and C_{lin}.

The values of the parameters identified using this three-step procedure are listed in Table 1. This table illustrates that weak coupling was indeed realized, and that the nonlinearity was essential as C_{lin} is negligible

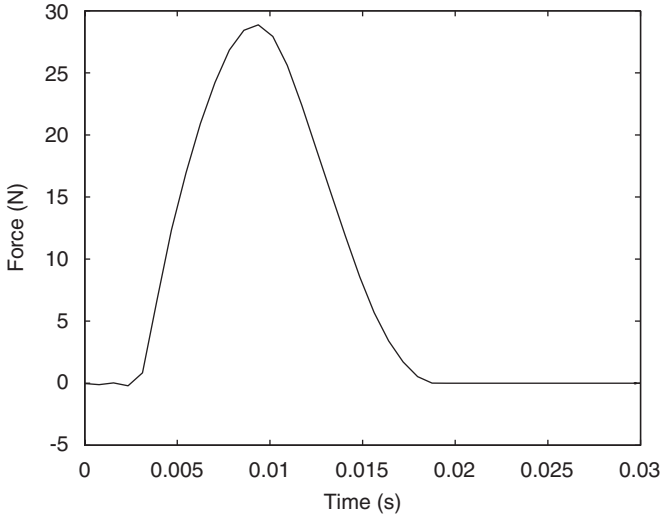

Fig. 4. Measured impulsive force.

Table 1
System parameters identified using modal analysis and the restoring force surface method

Parameter	Value
Mass of the primary system, M	0.7348 kg
NES mass, m	0.4734 kg
Stiffness of the primary system, k_1	942 N/m
Coupling stiffness, k_{12}	151 N/m
Damper of the primary system, c_1	0.09 Ns/m
NES damper, c_2	0.11 Ns/m
Coupling damper (tape), c_{12}	0.4 Ns/m
Cubic stiffness, C	1.83×10^7 N/m^3
Linear stiffness, C_{lin}	11.3 N/m

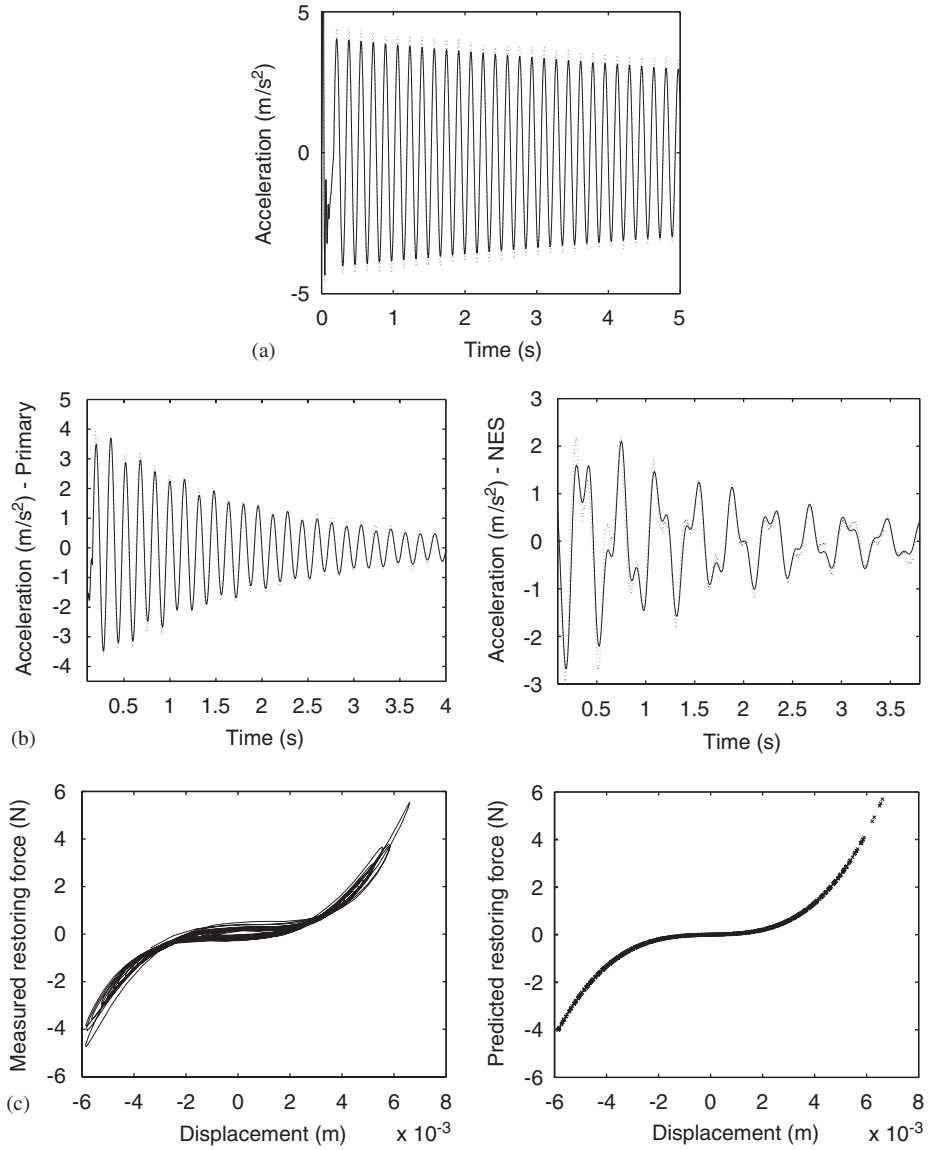

Fig. 5. Accuracy of system identification (3 steps). (a) Step 1: modal analysis of the primary system only (solid line: measured acceleration; dotted line: acceleration predicted by the identified model); (b) step 2: modal analysis of the coupled system without the nonlinearity (solid line: measured acceleration; dotted line: acceleration predicted by the identified model); (c) step 3: nonlinearity identification using the restoring force surface method: measured and predicted restoring forces.

when compared to C. The predictions given by the identified model are compared to the measurements in Fig. 5, which demonstrates the accuracy of the identification.

3. Interpretation of the experimental results

Three excitation levels are considered herein, corresponding to peak amplitudes of 7, 13 and 18 N, respectively. Figure 6 displays the displacements of the primary system and the NES; for the sake of clarity, closes-up of the comparison of the displacements are also given in this figure. Overall, the NES displacement is higher than that of the primary system, which indicates that the NES participates in the system dynamics to a large extent. The system response at the 7 N level is qualitatively different from those at the other two levels.

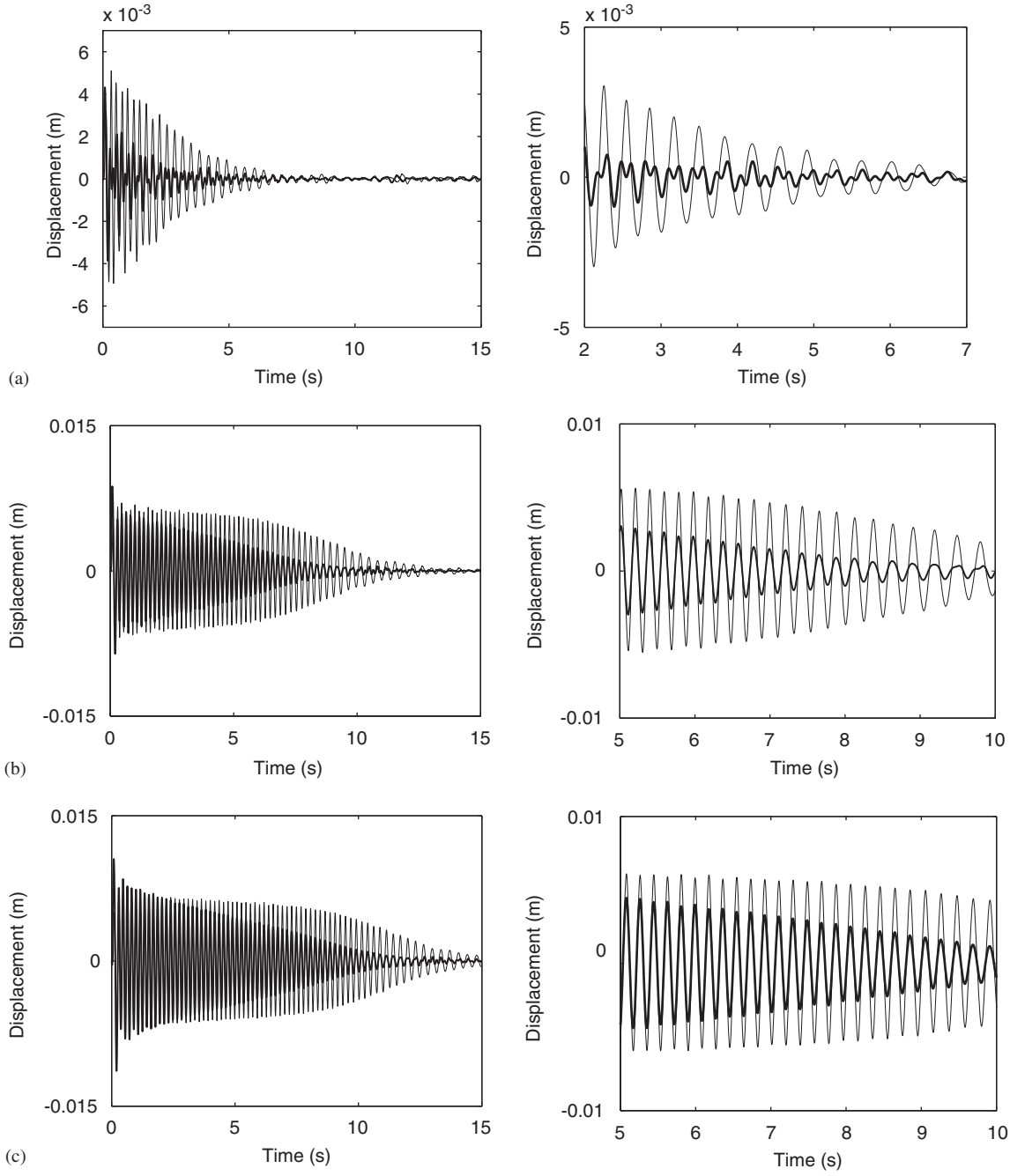

Fig. 6. Measured displacements for: (a) 7 N peak force; (b) 13 N peak force; (c) 18 N peak force (thick line: primary system; thin line: NES). Left column: entire record; right column: close-up.

At the 7 N level, the displacement of the primary system carries at least two significant frequency components, whereas the displacements at the 13 and 18 N levels are mainly monochromatic.

As clearly evident in the close-up, the two oscillators at the 13 and 18 N levels vibrate in an in-phase fashion with the same apparent frequency. The dynamical flow therefore seems to be captured in the neighborhood of a 1:1 resonance manifold. The transient nature of the resonance capture is not obvious from these plots but

will be clearly seen in the remainder of this study. An interesting feature of TRC is that the envelope of both displacement signals decreases monotonically during this regime, but the envelope of the NES seems to decrease more slowly than that of the primary system. This is a sign that energy transfer from the primary system to the NES takes place during TRC. Such a clean and prolonged 1:1 resonance was not observed in previous studies [22,23]. At this point, we also mention that no manual tuning of the nonlinear attachment was performed; the resonance occurs because the NES has no preferential resonant frequency.

Further evidence of the resonance capture is given in Fig. 7, which depicts the instantaneous frequencies of the measured displacements computed using a wavelet transform. Darkly shaded areas correspond to regions where the amplitude of the wavelet transform is high, which reveals the presence of a significant frequency component, whereas lightly shaded regions correspond to low amplitudes. Figs. 7(b) and (c) clearly indicate that the two oscillators vibrate with the same frequency; they are in a state of 1:1 resonance whose captured frequency shifts downward (due to the hardening characteristic of the nonlinearity) as the total energy of the system is reduced by viscous dissipation. This decrease in frequency is particularly important because at the beginning and at the end of TRC the frequency is around the natural frequency of the linear oscillator (i.e., 5.7 Hz and 3.3 Hz, respectively). Finally, note that the presence of two significant frequency components in the displacement of the primary system at the 7 N level is evident in Fig. 7(a).

Another means of studying resonance capture is to monitor the phase difference $\Phi_{12}(t)$ between the two oscillators. This was carried out in the literature using the method of averaging [6], harmonic balance-based averaging [16] or a complexification technique [7,11]. In the neighborhood of a resonance manifold, a non-time-like behavior of the phase variable occurs, which prevents direct averaging of the equations of motion over this phase difference (being treated as a 'fast' or 'time-like' independent variable); the failure of the averaging theorem is due to the vanishing of a denominator in the averaged equations or, equivalently, to the slow variation of the phase difference between the two oscillators. In the present study, the phase difference between the oscillators is computed directly from the experimental responses using the Hilbert transform $H[\bullet]$. The analytic signal $X(t)$ corresponding to a real-valued signal $x(t)$ can be represented using the Hilbert transform as a combination of slowly varying functions, called the envelope $A(t)$ and the instantaneous phase $\Phi(t)$ [25]

$$X(t) = x(t) + \mathrm{j}H[x(t)] = A(t)\exp[\mathrm{j}\Phi(t)] \tag{4}$$

with

$$x(t) = A(t)\cos\Phi(t), \quad A(t) = \sqrt{x(t)^2 + H[x(t)]^2}, \tag{5}$$

$$\mathrm{j} = \sqrt{-1}, \quad \Phi(t) = \arctan[H[x(t)]/x(t)] \tag{6}$$

The instantaneous frequency is the time derivative of the instantaneous phase. The investigation of the vibrations of nonlinear systems using this procedure was proposed by Feldman [26].

The temporal evolution of the phase difference $\Phi_{12}(t) = \Phi(t) - \Psi(t)$, where $y(t) = A(t)\cos\Phi(t)$ and $v(t) = B(t)\cos\Psi(t)$, and its trajectory in the phase plane are depicted in Fig. 8. In Figs. 8(b) and (c), a non-time-like behavior of the phase difference is observed which is followed at around $t = 10$ s by a time-like behavior of $\Phi_{12}(t)$. These are a clear indication of resonance capture and escape from resonance capture, respectively, and emphasize the transient nature of the resonance capture. The small oscillations of the phase difference around 0 confirm that the oscillators are in-phase during TRC.

Focusing now on Fig. 8(a), we note a completely different behavior. The previous procedure cannot be applied in this case because the displacement of the primary system possesses multiple frequency components, which violates the assumption that $y(t) = A(t)\cos\Phi(t)$. An extension of this procedure in the case of multiple frequency components was developed by Huang and co-authors [27]. In essence, the proposed methodology consists of decomposing a signal $x(t)$ in terms of intrinsic mode functions (IMFs); thus, $x(t) = \sum_i \mathrm{IMF}_i(t)$

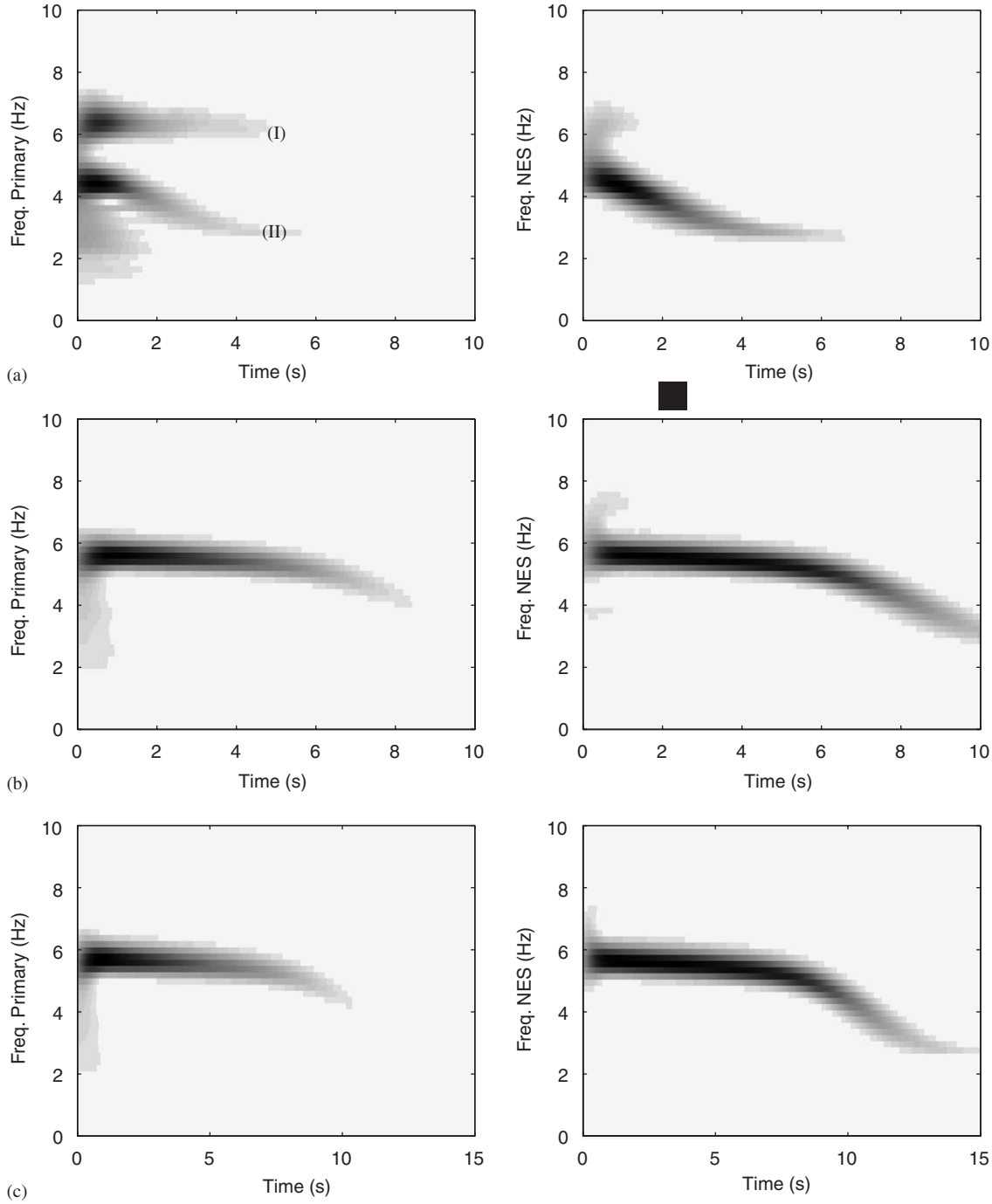

Fig. 7. Instantaneous frequencies of the measured displacements computed using the wavelet transform for: (a) 7 N peak force; (b) 13 N peak force; (c) 18 N peak force (I, II: two dominant harmonic components). Left column: primary system; right column: NES.

(each IMF must have the same number of extrema and zero-crossings and only one extremum between successive zero-crossings). Doing so, the previous procedure can be applied to each IMF individually. A complete description of the method is beyond the scope of this paper; the interested reader may consult reference [27] for further details.

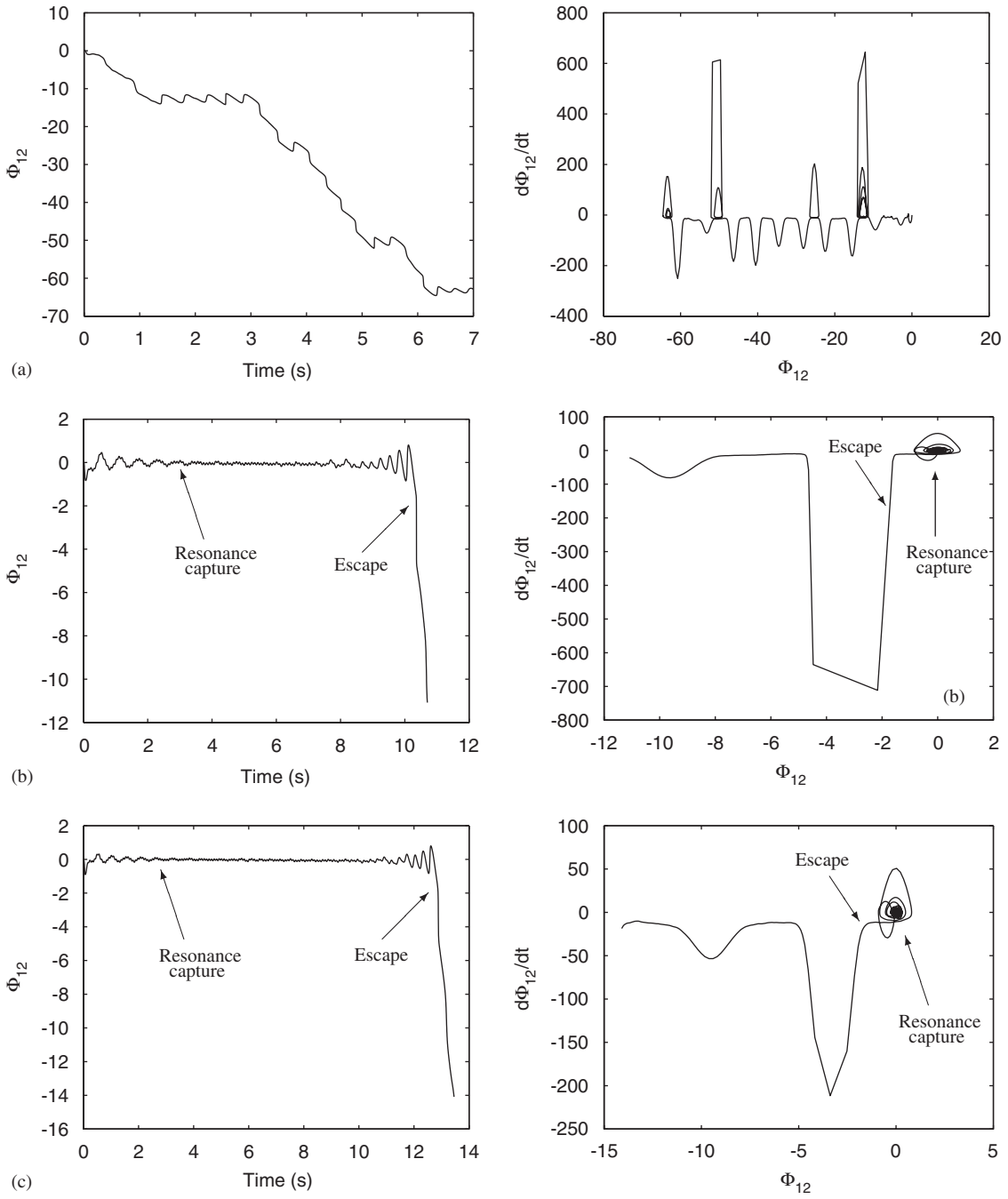

Fig. 8. Phase modulations and their trajectories for: (a) 7 N peak force; (b) 13 N peak force; (c) 18 N peak force. Left column: phase modulations; right column: trajectories of the phase modulations.

Fig. 9 shows the first two IMFs computed from the displacement of the oscillators; higher-order IMFs were also computed but had a negligible participation in the system response. For the primary system [see Fig. 9(a)], the two IMFs have approximately the same contribution to the system response, which indicates that $y(t) \cong \mathrm{IMF}_1(t) + \mathrm{IMF}_2(t) = A_1(t)\cos\Phi_1(t) + A_2(t)\cos\Phi_2(t)$. The first and second IMFs correspond to components I and II in Fig. 7(a), respectively. On the other hand, the second IMF of the

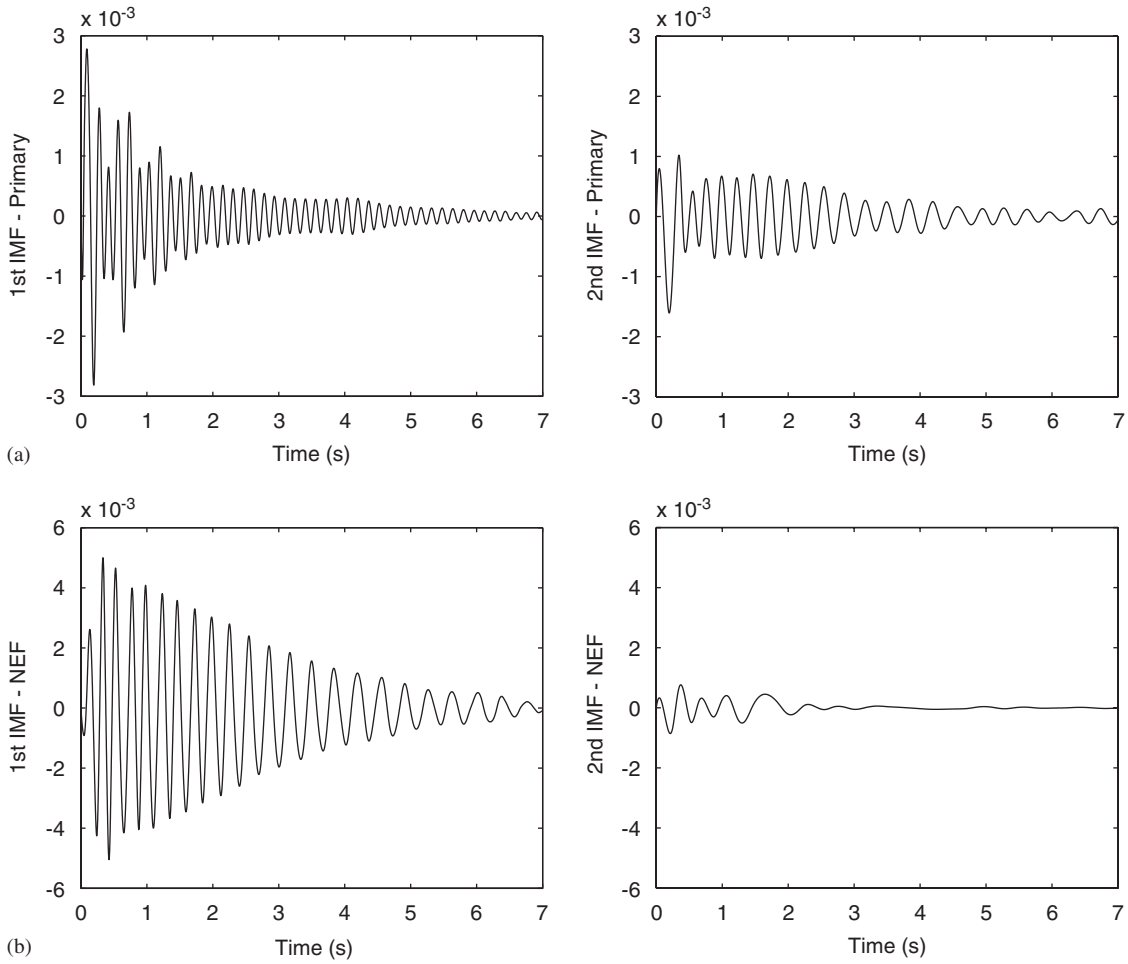

Fig. 9. Huang–Hilbert transform (7 N) for: (a) primary system; (b) NES. Left column: first IMF; right column: second IMF.

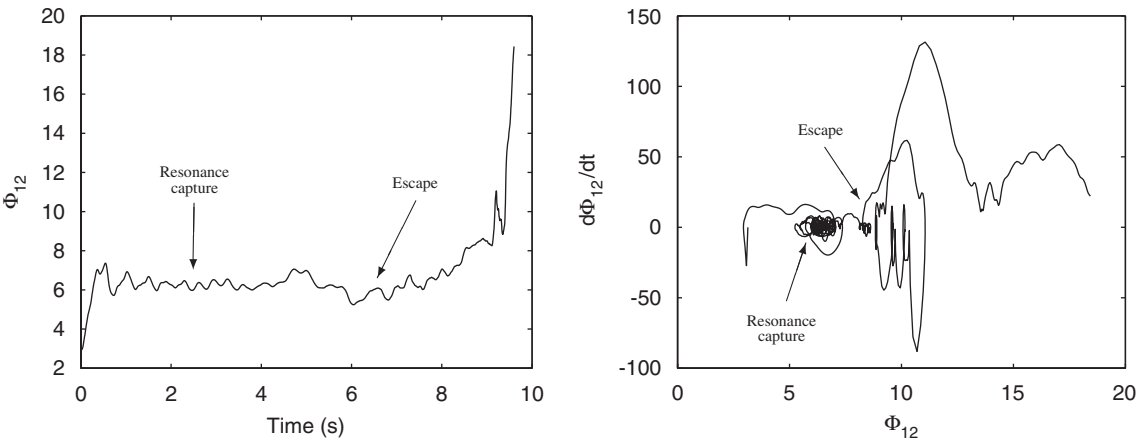

Fig. 10. Phase modulation and its trajectory. Left plot: phase modulation between the second IMF of the displacement of the primary system and the first IMF of the NES diplacement (7 N); right plot: trajectory of the phase modulation.

NES displacement can be neglected when compared to the first IMF [see Fig. 9(b)]; as a result, $v(t) \cong \mathrm{IMF}_1(t) = B_1(t)\cos\Psi_1(t)$.

A close look at Fig. 9 reveals that the second IMF of the displacement of the primary system, $A_2(t)\cos\Phi_2(t)$, and the first IMF of the NES displacement, $B_1(t)\cos\Psi_1(t)$, have the same frequency content; their phase difference, $\Phi_2(t) - \Psi_1(t)$, is displayed in Fig. 10(a). This graph shows that this particular phase difference has a non-time-like behavior at least until at time of 4–5 s. The low-frequency components of the displacements of the two oscillators are therefore in resonance. However, there is no such observation for the phase difference between the first IMF of the displacement of the primary system and the second IMF of the NES displacement, which explains why overall TRC cannot be observed at the 7 N level.

The left column of Fig. 11 presents the instantaneous percentage of total energy carried by the NES

$$E_{\mathrm{NES},\%}(t) = 100\frac{E_{\mathrm{NES}}(t)}{E_{\mathrm{Prim}}(t) + E_{\mathrm{NES}}(t)} \tag{7}$$

$$= 100\frac{m\dfrac{\dot{v}^2(t)}{2} + C\dfrac{v^4(t)}{4} + k_{12}\dfrac{[y(t)-v(t)]^2}{2}}{M\dfrac{\dot{y}^2(t)}{2} + k_1\dfrac{y^2(t)}{2} + m\dfrac{\dot{v}^2(t)}{2} + C\dfrac{v^4(t)}{4} + k_{12}\dfrac{[y(t)-v(t)]^2}{2}} \tag{8}$$

for the three excitation levels, and illustrates that vigorous energy exchanges take place between the two oscillators. Again, the dynamics are completely different between the lowest level, 7 N, and the other two levels:

- At the lowest level, for which previous results indicated that TRC is not realized, a single regime can be observed during which energy quickly flows back and forth between the two oscillators. After 0.35 s, as much as 98.2% of the total energy is transferred from the impulsively loaded primary system to the NES, but this number drops to 18% immediately thereafter. Clearly, there is a nonlinear beat phenomenon, which is studied in detail in Refs. [11,28]. In Ref. [11], it is shown that this phenomenon may lead to vigorous but reversible energy transfer and that it may act as a 'bridging mechanism' (or 'catalyst') for triggering nonlinear energy pumping while the NES is at rest. Ref. [28] demonstrates that the excitation of periodic or quasiperiodic impulsive orbits are responsible for those nonlinear beats. It is important to note that no a priori tuning of the NES is necessary, which is markedly different from other systems exhibiting nonlinear beating phenomena (see, e.g., Ref. [2] or spring-pendulum systems).
- At the other two levels, for which a 1:1 TRC is realized, three regimes, labeled I, II and III, exist. During Regime I, a nonlinear beat phenomenon can also be observed during the first few cycles (though less vigorous than at the 7 N level). Although this regime could not be clearly observed in Figs. 6–8, except for the presence of small harmonic components in Figs. 7(b) and (c), it plays a very important role as it brings the motion into the domain of attraction of the 1:1 resonance manifold by transferring some energy to the NES. The system is then capable of sustaining a 1:1 TRC during a large part of the motion, namely, during Regime II. This was thoroughly discussed in Refs. [8,11] using numerical examples. From Fig. 11, it is evident that another manifestation of TRC in coupled oscillators with essential nonlinearity is that targeted nonlinear energy transfers take place. At the beginning of Regime III, the NES carries almost all the instantaneous total energy; then escape from resonance capture occurs, and energy is released from the NES back to the primary system. It is important to note that when this occurs the total energy level is small compared to the initial value.

The right column of Fig. 11 presents the energy dissipated in the NES normalized by the total input energy,

$$E_{\mathrm{diss}}(t) = \frac{c_{12}\int_0^t[\dot{v}(\tau)-\dot{y}(\tau)]^2\,\mathrm{d}\tau + c_2\int_0^t[\dot{v}(\tau)]^2\,\mathrm{d}\tau}{\int_0^{t_{\max}} p(\tau)\dot{y}(\tau)\,\mathrm{d}\tau} \tag{9}$$

and indicates that, eventually, the NES is responsible for the dissipation of a great portion of the total energy imparted to the system.

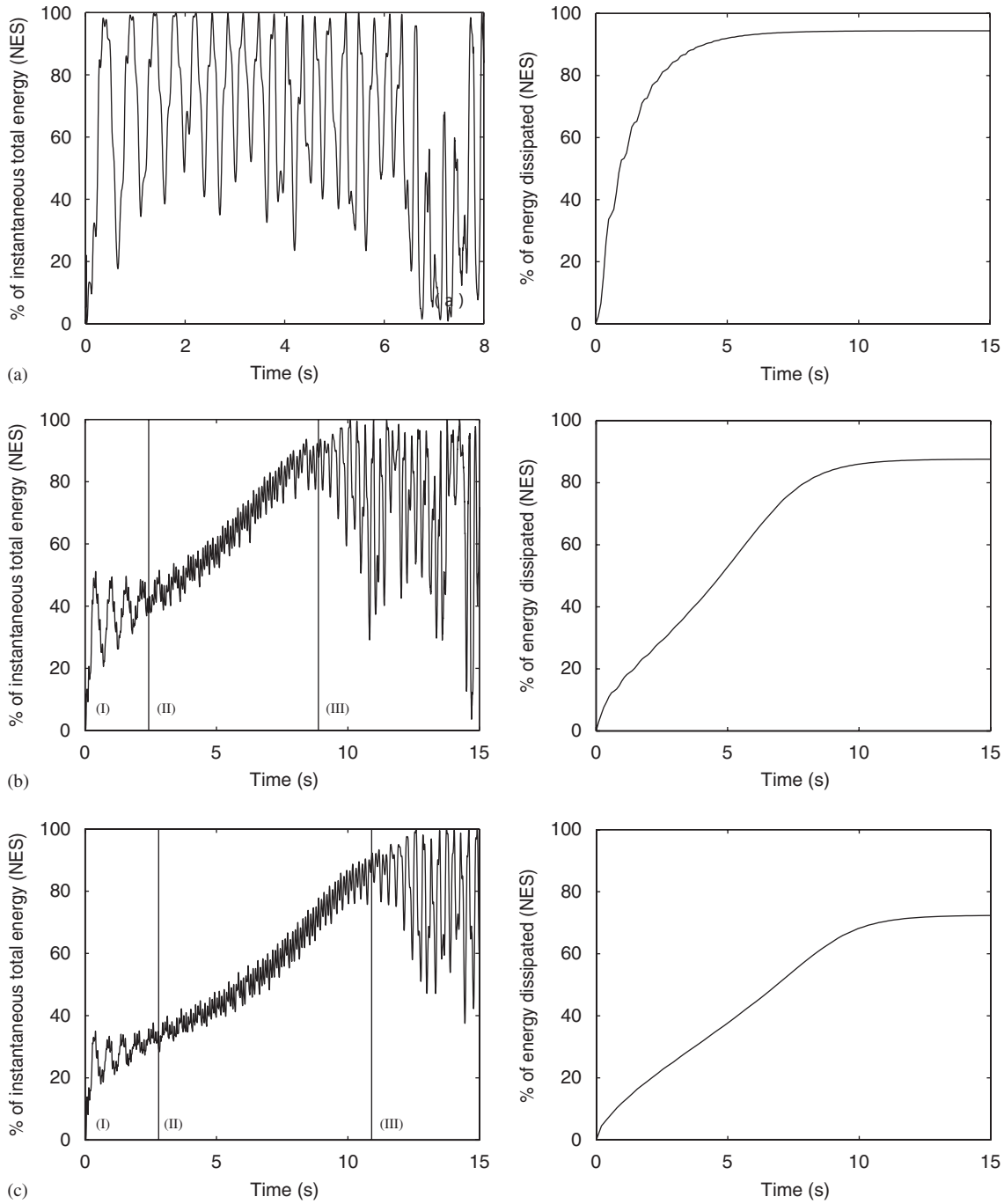

Fig. 11. Distribution of energy as a function of time for: (a) 7 N peak force; (b) 13 N peak force; (c) 18 N peak force. Left column: percentage of instantaneous total energy in the NES (Regime I: nonlinear beat phenomenon; regime II: resonance capture; regime III: escape from resonance capture); right column: energy dissipated in the NES.

In Ref. [8], it was shown that the structure and bifurcations of the periodic orbits of the undamped and unforced system enable one to understand the energy transfers in the weakly damped and impulsively loaded system. All the computed periodic orbits were gathered in a frequency-energy plot. By studying the motion on

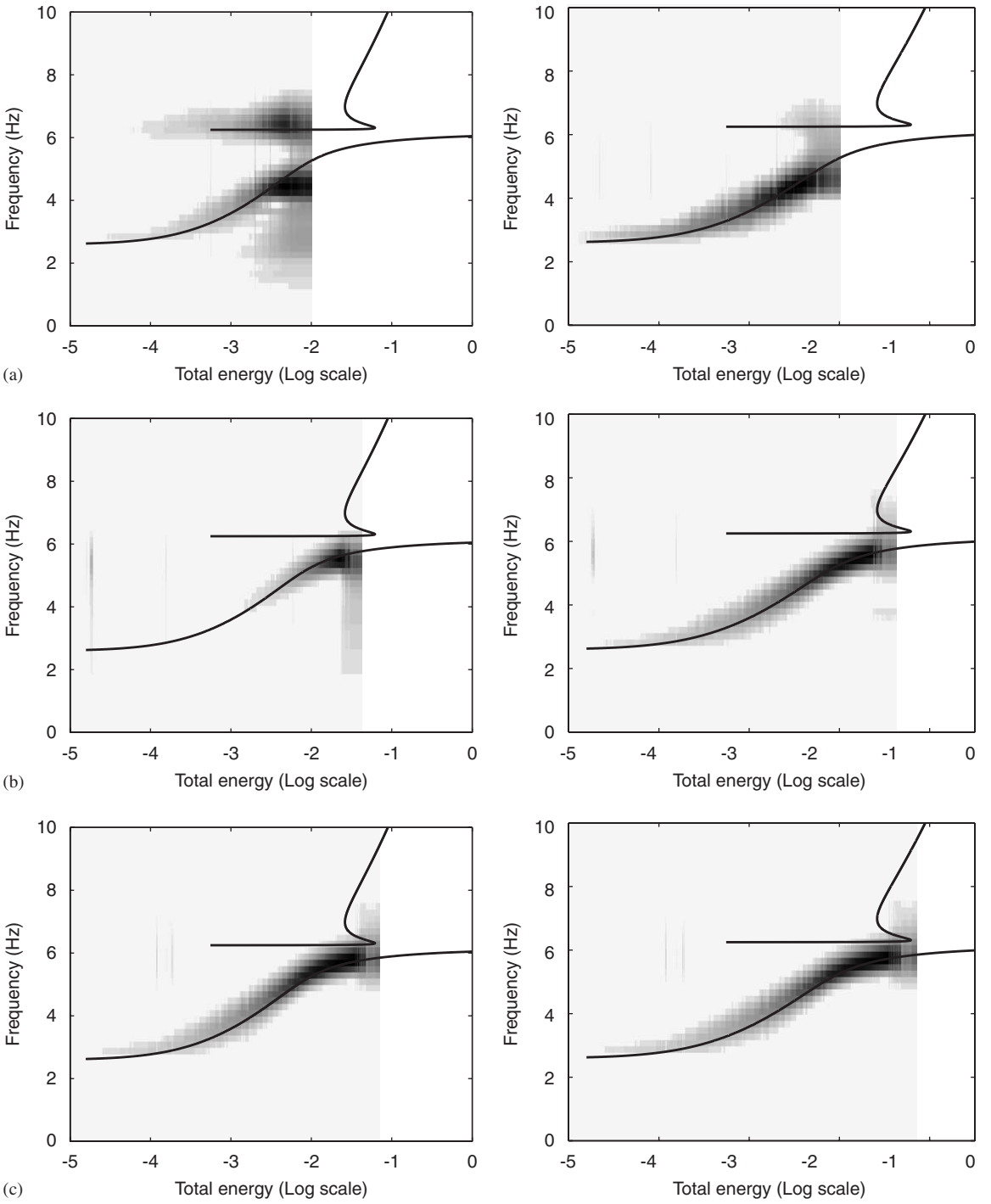

Fig. 12. Wavelet transform of the displacements superposed on the frequency-energy plot for: (a) 7 N peak force; (b) 13 N peak force; (c) 18 N peak force. Left column: primary system; right column: NES.

one of the two branches building the backbone of the frequency-energy plot, it became clear that a 1:1 TRC leads to targeted nonlinear energy transfers. To illustrate all this, the wavelet transforms of Fig. 7 can also be represented in a frequency-energy plane by substituting the instantaneous energy in the system for time. In Fig. 12, the backbone curve of the frequency-energy plot, represented by a solid line and computed using the

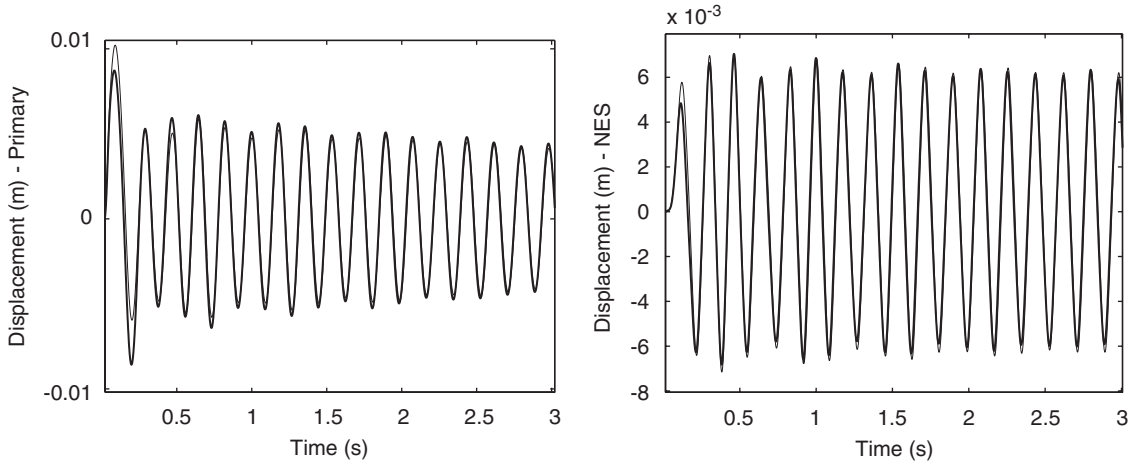

Fig. 13. Comparison between measured and predicted displacements (13 N; thick line: measurements; thin line: predictions). Left plot: primary system; right plot: NES.

undamped version of Eqs. (1) with the experimentally identified parameter values, is superposed on the wavelet transforms of the measured displacements. This plot is a schematic representation because it superposes damped (the wavelet transform) and undamped (the frequency-energy plot) responses and is used for descriptive purposes only. However, it represents a useful tool for the interpretation of the dynamics. It indicates that:

- For all three excitation levels, the predominant frequency components follow a backbone branch for most of the signal. This validates our conjecture that the weakly damped, transient dynamics can be interpreted mainly in terms of the periodic orbits of the underlying Hamiltonian system.
- The dynamics of the system is strongly nonlinear, as the predominant frequency components undergo significant variations with energy.
- During a 1:1 TRC, the displacements of both oscillators contain mainly one frequency component which closely follows the lower part of the backbone branch [see Figs. 12(b) and (c)]. At the 7 N level, for which a vigorous nonlinear beat phenomenon was observed, there are two frequency components, one of which closely follows the horizontal portion of the upper backbone curve while the other follows the lower backbone branch.

Finally, as in Refs. [22,23], satisfactory agreement was obtained between analytical and computational predictions and experimental measurements throughout this study, this in spite of the transient and strongly nonlinear nature of the NES dynamics. For illustration, a comparison between the measured displacements and the displacements predicted through numerical integration of Eqs. (1) with the experimentally identified parameter values is given in Fig. 13.

4. Concluding remarks

Two different kinds of resonance captures, SRC (sustained) and TRC (transient), were reported in the literature. In this paper, an experimental investigation of a 1:1 TRC in a system of two coupled oscillators with essential nonlinearity was performed. The lack of any preferential frequency of the NES makes it able to engage in TRC with the linear oscillator. The main findings from this study are:

- The resonance capture was termed transient (TRC) because it can be sustained only during some part of the motion; eventually, escape from resonance capture occurs.
- The existence of TRC is conditional upon the amplitude of the impulsive load.

- During TRC, the two oscillators vibrate with the same frequency; however, the captured frequency shifts downward with time due to the hardening characteristic of the nonlinearity.
- During TRC, the phase difference between the two oscillators has a non-time-like behavior.
- During TRC, one-way and irreversible energy transfers from the linear oscillator to the nonlinear attachment take place.

The use of the Hilbert transform or the Huang–Hilbert transform in the case of multifrequency response signals is proposed for the investigation of nonlinear resonances in practical applications. The procedure developed here will form the basis of further studies with increased dimensionality [29].

Finally, let us point out that the damping was kept relatively low in order to highlight the different dynamical phenomena. TRC in systems possessing increased damping will be examined in subsequent studies.

Acknowledgments

This work was funded in part by AFOSR Contracts F49620-01-1-0208 and 00-AF-B/V-0813.

One of the authors (GK) is supported by a grant from the Belgian National Fund for Scientific Research (FNRS), which is gratefully acknowledged. This study was carried out while GK was a postdoctoral fellow at the University of Illinois. The support of the Fulbright and Duesberg Foundations, which made his visit possible, is also gratefully acknowledged.

References

[1] L. Meirovitch, *Analytical Methods in Vibrations*, The Macmillan Co., New York, 1967.
[2] A.H. Nayfeh, D. Mook, *Nonlinear Oscillations*, Wiley Interscience, New York, 1984.
[3] J.A. Sanders, On the passage through resonance, *SIAM Journal of Mathematical Analysis* 10 (1979) 1220–1243.
[4] R. Haberman, Energy bounds for the slow capture by a center in sustained resonance, *SIAM Journal of Applied Mathematics* 43 (1983) 244–256.
[5] V.I. Arnold, *Dynamical Systems III (Encyclopaedia of Mathematical Sciences)*, Springer, Berlin, 1988.
[6] A. Zniber, D. Quinn, Frequency shifting in nonlinear resonant systems with damping, in: *Proceedings of the 2003 ASME Design Engineering Technical Conferences*, Chicago, 2003, DETC2003/VIB-48444.
[7] A.F. Vakakis, O. Gendelman, Energy pumping in nonlinear mechanical oscillators: part II—resonance capture, *Journal of Applied Mechanics* 68 (2001) 42–48.
[8] G. Kerschen, A.F. Vakakis, Y.S. Lee, D.M. McFarland, J.J. Kowtko, L.A. Bergman, Energy transfers in a system of two coupled oscillators with essential nonlinearity: 1:1 resonance manifold and transient bridging orbits, *Nonlinear Dynamics* 42 (2005) 283–303.
[9] D.D. Quinn, Capture, nonlinear normal modes, and energy transfer through non-stationary resonances, in: *Second International Conference on Nonlinear Normal Modes and Localization in Vibrating Systems*, Samos, Greece, 2006.
[10] Y.S. Lee, G. Kerschen, A.F. Vakakis, P. Panagopoulos, L.A. Bergman, D.M. McFarland, Complicated dynamics of a linear oscillator with an essentially nonlinear local attachment, *Physica D* 204 (2005) 41–69.
[11] G. Kerschen, Y.S. Lee, A.F. Vakakis, D.M. McFarland, L.A. Bergman, Irreversible passive energy transfer in coupled oscillators with essential nonlinearity, *SIAM Journal of Applied Mathematics* 66 (2006) 648–679.
[12] A.F. Vakakis, D.M. McFarland, L.A. Bergman, L.I. Manevitch, O. Gendelman, Isolated resonance captures and resonance capture cascades leading to single- or multi-mode passive energy pumping in damped coupled oscillators, *Journal of Vibration and Acoustics* 126 (2004) 235–244.
[13] D. Quinn, R. Rand, J. Bridge, The dynamics of resonance capture, *Nonlinear Dynamics* 8 (1995) 1–20.
[14] R. Haberman, R. Rand, T. Yuster, Resonant capture and separatrix crossing in dual-spin spacecraft, *Nonlinear Dynamics* 18 (1999) 159–171.
[15] R. Mankala, D. Quinn, Resonant dynamics and saturation in a coupled system with quadratic nonlinearities, in: Proceedings of the 2004 ASME International Mechanical Engineering Congress, Anaheim, 2004, IMECE2004-61623.
[16] K. Nandakumar, A. Chatterjee, The simplest resonance capture problem using harmonic balance based averaging, *Nonlinear Dynamics* 37 (2004) 271–284.
[17] D.L. Vainchtein, E.V. Rovinsky, L.M. Zelenyi, A.I. Neishtadt, Resonances and particle stochastization in nonhomogeneous electromagnetic fields, *Journal of Nonlinear Science* 14 (2004) 173.
[18] R. Fux, Order and chaos in the local disc stellar kinematics induced by the galactic bar, *Astronomy and Astrophysics* 373 (2001) 511–535.
[19] E. Gourdon, C.H. Lamarque, Energy pumping with various nonlinear structures: numerical evidences, *Nonlinear Dynamics* 40 (2005) 281–307.

[20] O.V. Gendelman, D.V. Gorlov, L.I. Manevitch, A.I. Musienko, Dynamics of coupled linear and essentially nonlinear oscillators with substantially different masses, *Journal of Sound and Vibration* 286 (2005) 1–19.
[21] Y.S. Lee, A.F. Vakakis, L.A. Bergman, D.M. McFarland, Elimination of limit cycle oscillation in a van der pol oscillator using a nonlinear energy sink, in: *Proceedings of the Third International Conference on Advances in Structural Engineering and Mechanics*, Seoul, Korea, 2006, pp. 330–339.
[22] D.M. McFarland, L.A. Bergman, A.F. Vakakis, Experimental study of nonlinear energy pumping occurring at a single fast frequency, *International Journal of Non-linear Mechanics* 40 (2005) 891–899.
[23] D.M. McFarland, G. Kerschen, J.J. Kowtko, Y.S. Lee, L.A. Bergman, A.F. Vakakis, Experimental investigation of targeted energy transfers in strongly and nonlinearly coupled oscillators, *Journal of the Acoustical Society of America* 118 (2005) 791–799.
[24] S.F. Masri, T.K. Caughey, A nonparametric identification technique for nonlinear dynamic systems, *Journal of Applied Mechanics* 46 (1979) 433–447.
[25] R.E. Ziemer, W.H. Tranter, *Principle of Communication: Systems, Modulation and Noise*, Houghton Mifflin, Boston, 1976.
[26] M. Feldman, Non-linear system vibration analysis using Hilbert transform—I. Free vibration analysis method 'freevib', *Mechanical Systems and Signal Processing* 8 (1994) 119–127.
[27] N.E. Huang, Z. Shen, S.R. Long, M.C. Wu, H.H. Shih, Q. Zheng, N.C. Yen, C.C. Tung, H.H. Liu, The empirical mode decomposition and the Hilbert spectrum for nonlinear and non-stationary time series analysis, *Proceedings of the Royal Society of London, Series A—Mathematical, Physical and Engineering Sciences* 454 (1998) 903–995.
[28] G. Kerschen, O. Gendelman, A.F. Vakakis, L.A. Bergman, D.M. McFarland, Impulsive periodic and quasi-periodic orbits in a system of coupled oscillators with essential stiffness nonlinearity, *Communications in Nonlinear Science and Numerical Simulation*, accepted for publication.
[29] F. Georgiadis, A.F. Vakakis, G. Kerschen, Broadband irreversible targeted energy transfer from a linear dispersive rod to a lightweight essentially nonlinear end attachment, *International Journal of Non-Linear Mechanics*, accepted for publication.